

EULER STUDIES ON 21463 RTA-70 CONFIGURATION USING HYENA

Vishal S. Shirbhate, Gopal K. Panda, Dr. J.S. Mathur
Computational & Theoretical Fluid Dynamics Division
Systems Engineering Division

Council of Scientific and Industrial Research - National Aerospace Laboratories,
Bangalore - 560017, Karnataka, India

ABSTRACT

The inviscid CFD studies are carried out using in-house Hyena code. The computations have been performed on various configurations of RTA-21463. The symmetric and asymmetric studies are carried out for wing-alone, wing-winglet, wing-winglet-body and wing-winglet-body-empennage models. All the computations are carried out for various Mach numbers. The side-slip cases are studied for various β ranging from 2.5° to 10° for a $AOA=3^\circ$ and 5° . The winglet has shown improvement over wing-alone case. The code Hyena can be used further for Drag Divergence Analysis.

Keywords: CFD, Euler, Aerodynamics, Unstructured Mesh, Side-Slip Angle, Hyena

INTRODUCTION

Today's aerospace industry mainly relies on Computational Fluid Dynamics (CFD) tool for a successful aerodynamic design of any type of aircraft as it quickly provides the aerodynamic force and moment coefficient with reasonable accuracy. For the safe and precise deployment of personnel and material, a deep understanding of the flow physics for the corresponding flight conditions and geometries are necessary. Since the aircraft is still under development, the tools to improve this understanding are so far restricted to experiments and numerical simulations. The current study deals with the 3D-Euler computations carried out for the different components of Regional Transport Aircraft viz. wing-alone, wing-winglet, wing-body, and wing-body-empennage. The work has also been carried out to understand the effect of side-slip angle. The main aerofoil designed for wing is nominated as RTA-21463.

OBJECTIVE

- 3D inviscid analysis for 21463 wing-alone (WA) configurations.
- 3D inviscid analysis for 21463 wing-winglet (WWL) configurations.
- 3D inviscid analysis for 21463 wing-body configuration (WBD) without side slip angle.
- 3D inviscid analysis for 21463 wing-body empennage configuration (WBDE) without side slip angle.
- 3D inviscid analysis for 21463 wing-body configuration (WBD) with side slip angle.
- 3D inviscid analysis for 21463 wing-body empennage (WBDE) configuration with side slip angle.

SAILANT FEATURES OF CODE HYENA

The Hyena code was originally developed in Aeronautical Development Agency in serial mode and a parallelization work of Hyena has been carried out in CTFD division of NAL. It is an explicit code and uses Advection Upstream Splitting Method (AUSM) scheme for convective flux discretization. It can handle mixed type of grids like hexahedral and a combination of tetrahedral & prism cells. It has been successfully validated in the design phase of Light Combat Aircraft (LCA) for a range of various Mach numbers.

GRID GENERATION:

The unstructured tetrahedral grid is used for all configurations. Commercial grid generation package ICEM-CFD is used as a grid generator for the current study. The volume domain is taken as 100 chord length for wing-alone and wing-winglet configuration whereas 10 counts of fuselage length for wing-body and wing-body-empennage configuration. The symmetry boundary condition is given at root of wing-alone and wing-winglet. The volume domain is considered as a far-field boundary condition. The grids for various configurations are shown in Fig.1. The grid is sufficiently refined around the fuselage fairing junction to capture the flow interference effects between these regions.

The grid sizes for different configurations are given below:

- i. 21463 wing-alone configuration = 0.87 million
- ii. 21463 wing-winglet configuration = 1.43 million
- iii. 21463 wing-body configuration (symmetric) = 1.55 million.
- iv. 21463 wing-body-empennage configuration (symmetric) = 1.66 million
- v. 21463 wing-body configuration (asymmetric) = 3.41 million.
- vi. 21463 wing-body-empennage configuration (asymmetric) = 5.32 million.

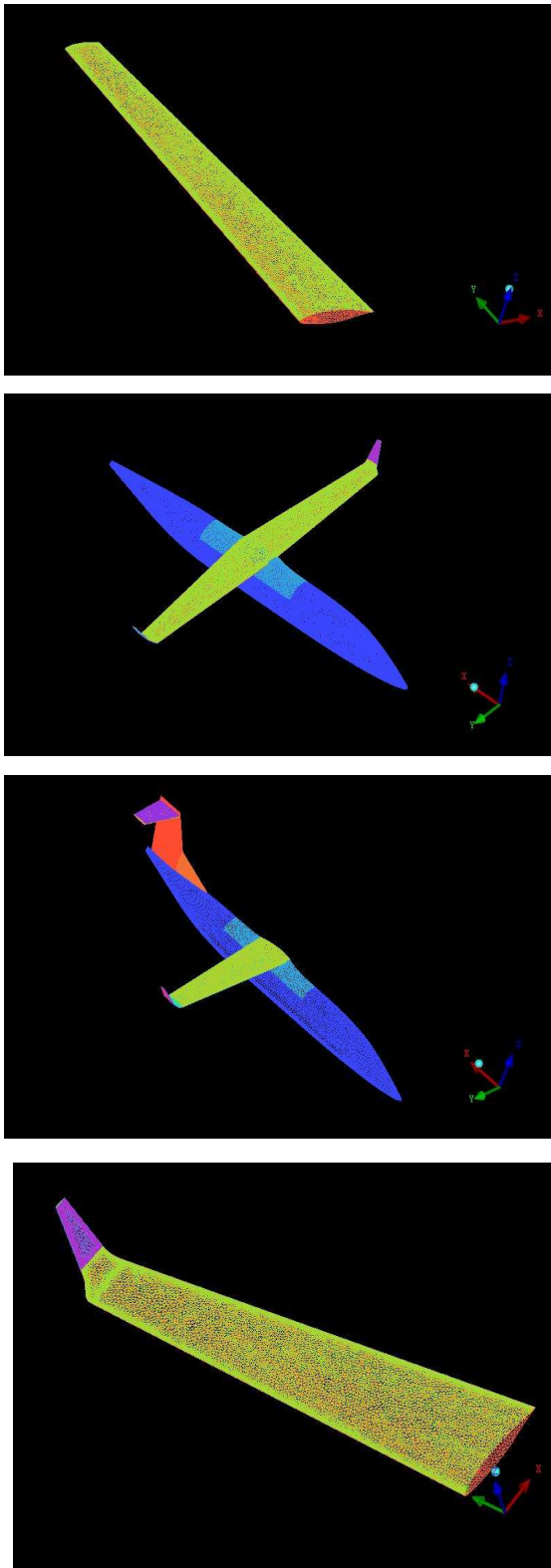


FIGURE 1

FLOW CONDITIONS:

The computations are carried out for different Mach numbers varying from 0.3, 0.5 and 0.7 with angle of attack ranging from -2° to 12° for the symmetry case. The asymmetrical case has been carried out for Mach number 0.7. The angle of attack and side slip angle used for present computations are tabulated in Table 1.

Mach Number	0.7
Angle of Attack (α) deg	3, 5
Side – Slip Angle (β) deg	0, 2.5, 5.0, 7.5, 9, 10, 11

The sign convention used for calculating moments are given below.

Rolling Moment (C_l) : +ve --Starboard Up

Yawing Moment (C_n) : -ve --towards Starboard

Pitching Moment C_m : +ve --Nose Down

RESULTS AND DISCUSSION:

The results obtained from the Euler computations are discussed the section for all the configurations.all computation are performed on SGI-ALTIX machine available at CSIR-4PI.

Symmetric Euler Computation

The angle of attack varies from -2° to 12° with increment of 2° . The Fig 6.1.a to Fig 6.2.c shows the lift coefficient versus angle of attack plot for various Mach numbers. The C_L is higher for winglet configuration as compared to wing-alone case which clearly tells the benefit of winglet. It also depicts the effects of lifting surfaces on the aircraft as the wing-body-empennage configuration predicts the highest C_L as the angle of attack tends to increase. Similarly, Fig. 6.2a to Fig 6.2.c describes the C_D variation for various angles of attack. The effect of winglet is also visible here with lowest drag observed for winglet configuration. The highest drag is observed for wing-body- empennage configuration. The curve tends to non-linearity at higher angles of attack for higher Mach numbers. It is also observed that the C_{L0} also increases with the increase in Mach number.

The Fi .6.3a to Fig.6.3b describes the C_L versus C_D for various Mach numbers. The improvement at $C_L= 0.55$ is found out to be 15.2% for $M=0.5$ which shows the benefit of the winglet over the wing-alone configuration.

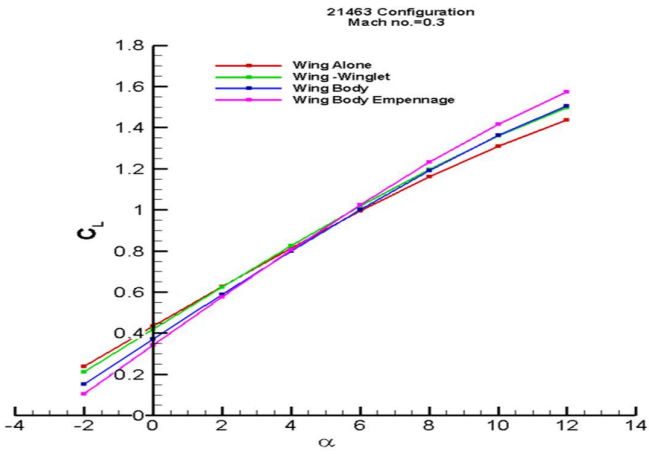


FIGURE: 6.1a.

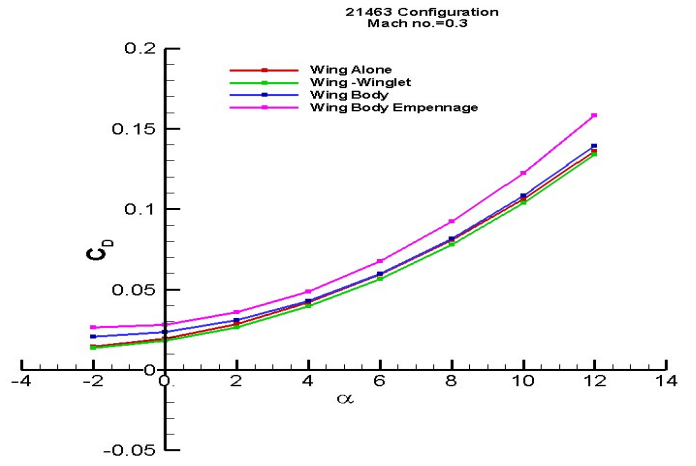


FIGURE: 6.2a.

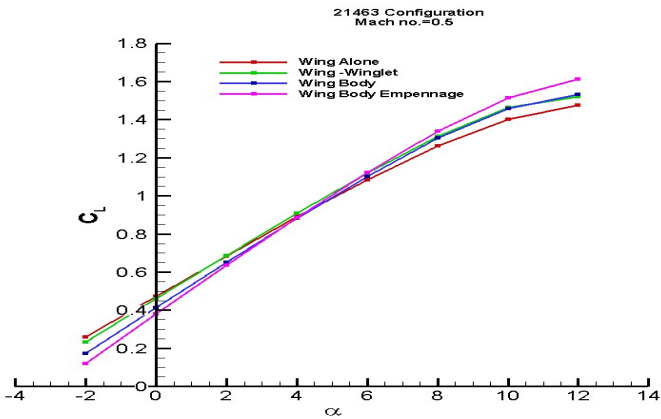


FIGURE: 6.1b.

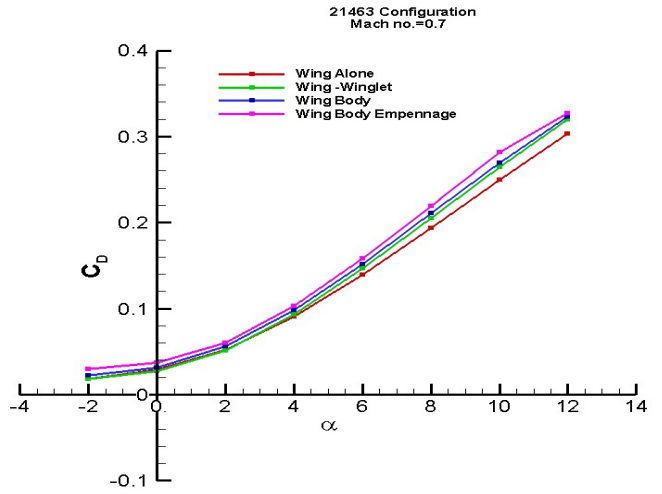


FIGURE: 6.2b.

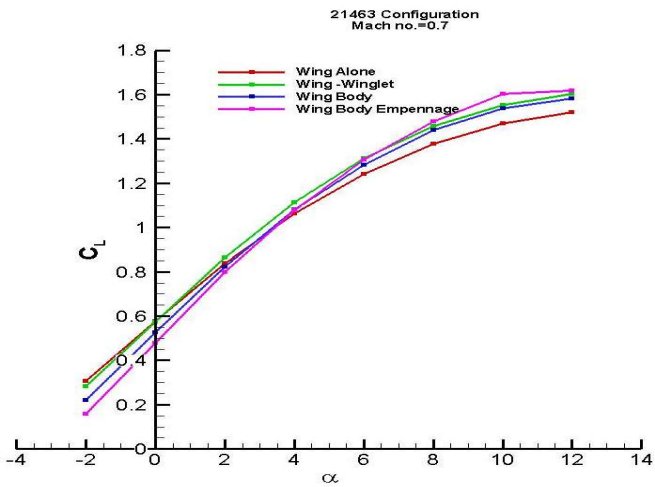


FIGURE: 6.1c.

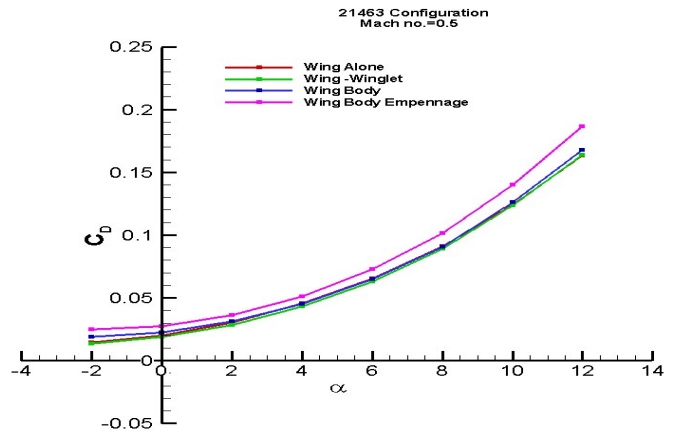


FIGURE: 6.2c.

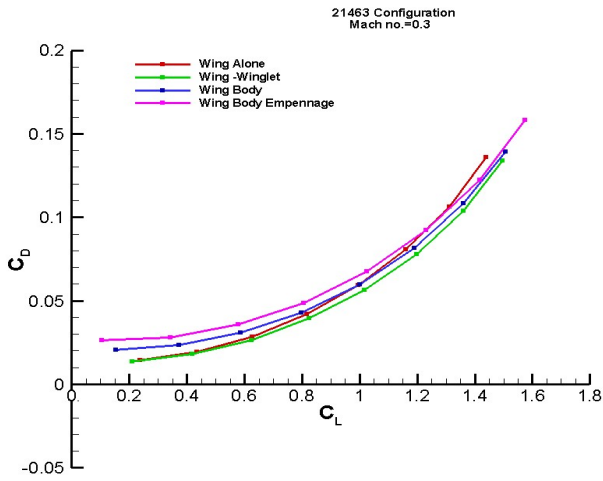


FIGURE: 6.3a.

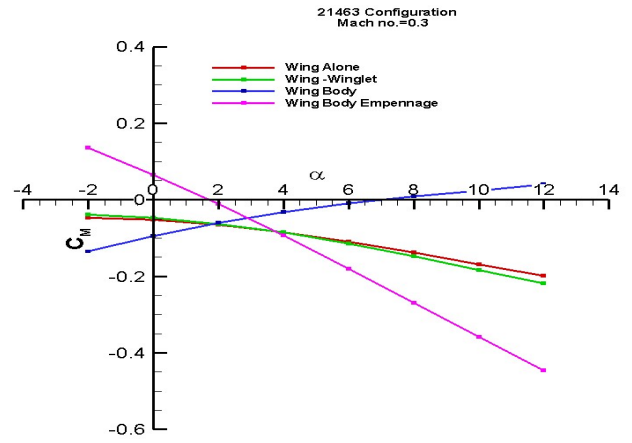


FIGURE: 6.4a.

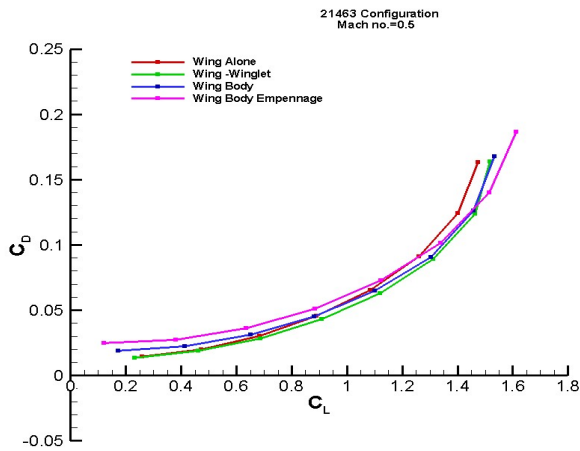


FIGURE: 6.3b.

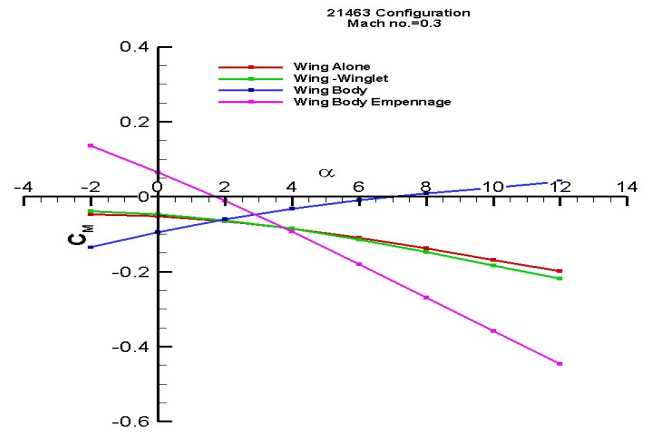


FIGURE: 6.4b.

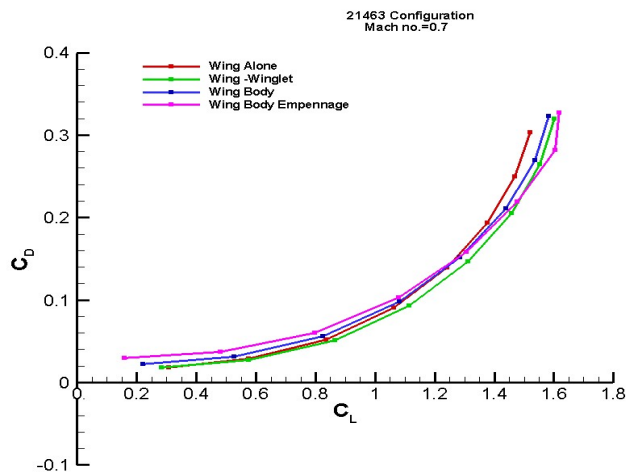


FIGURE: 6.3c.

The Fig.6.4.a to Fig.6.4.b shows the coefficient of pitching moment with respect to angle of attack for various Mach Numbers. The negative slope for positive α indicates stability in pitching. The Fig.6.5.a to Fig.6.5.c shows the behaviour of stability with respect to lift coefficient at various Mach numbers. It shows the CL_0 with respect to C_m increases with Mach Number for wing body and wing body empennage configuration.

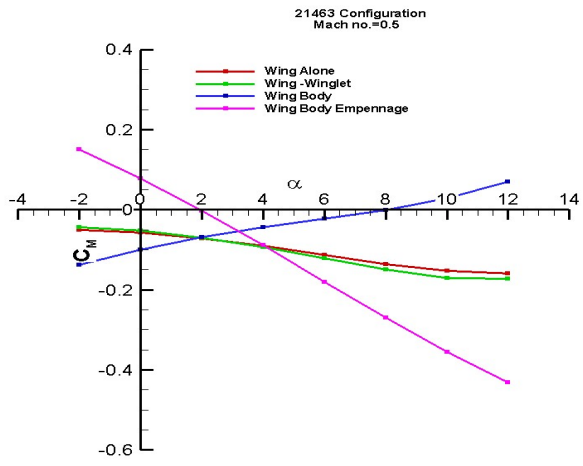


FIGURE: 6.4b

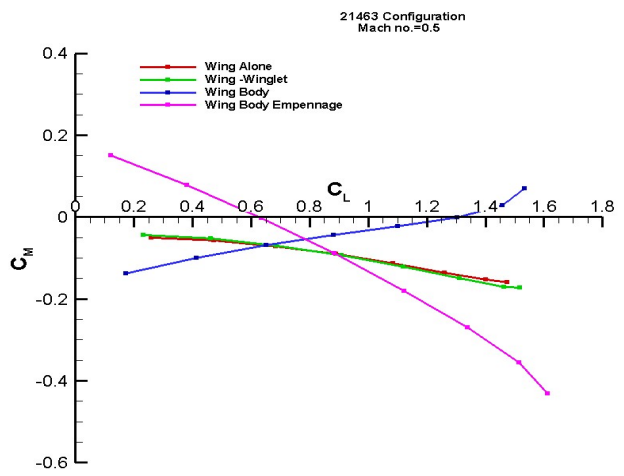


FIGURE: 6.5b

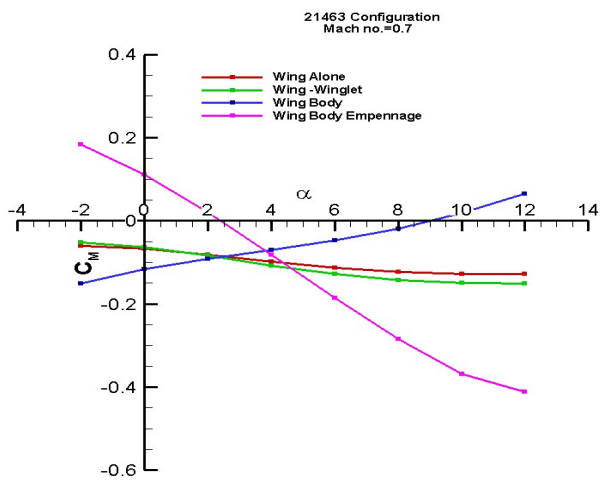


FIGURE: 6.4c

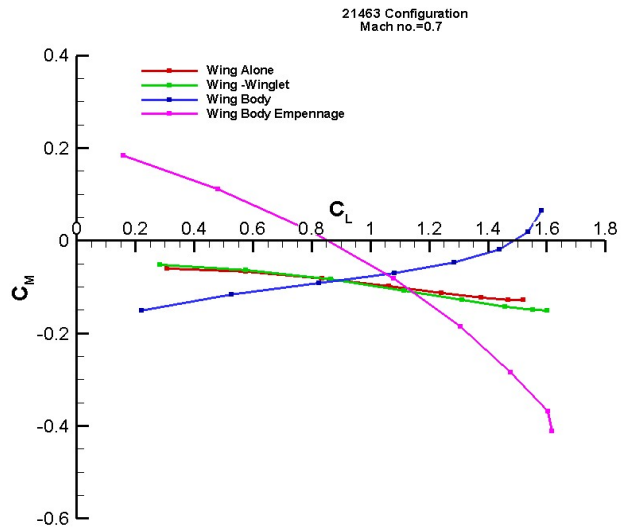


FIGURE: 6.5c.

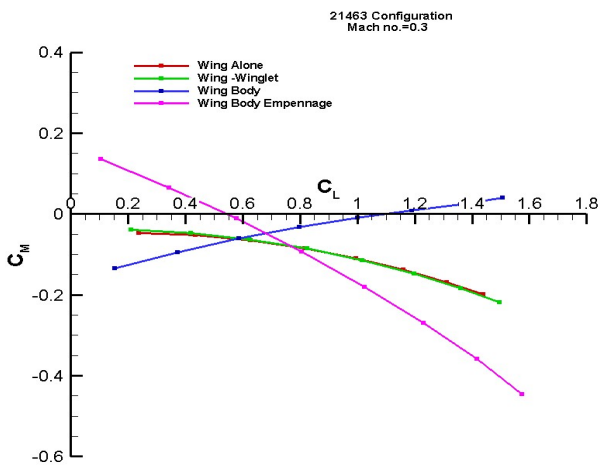


FIGURE: 6.5a.

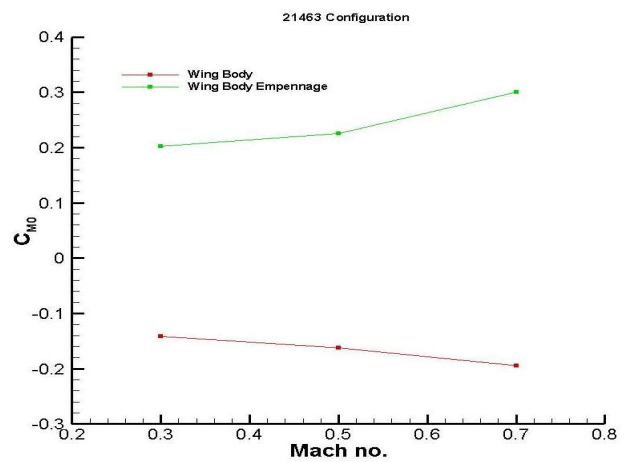


FIGURE: 6.6

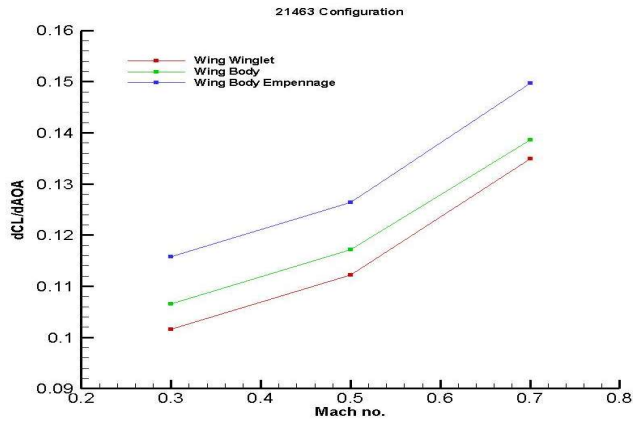


FIGURE: 6.7.

The Fig.6.6 depicts the C_{m_0} slope for wing body and wing body empennage at different Mach numbers. The negative slope in WBE indicates stability in pitching moment as expected. The Fig.6.7 depicts the C_L - α slope for wing-winglet, wing body and wing body empennage at different Mach numbers. The WBE predicts the highest slope numbers.

ASYMMETRIC EULER COMPUTATIONS

The asymmetric computation is carried out to check the behaviour of side slip angle on the RTA aircraft. The Fig.6.2.1 and Fig. 6.2.2 depicts the C_l - β graph for Mach Number 0.7 at $\alpha=3^\circ$ and 5° . The rolling moment shows increasing trend with respect to β as expected. At higher β , non-linearity has been observed which needs to be evaluated.

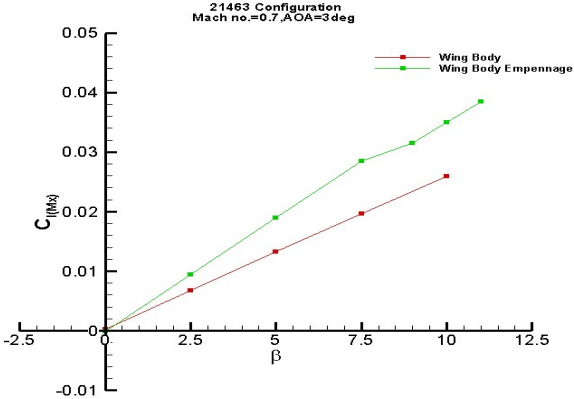


FIGURE: 6.2.1.

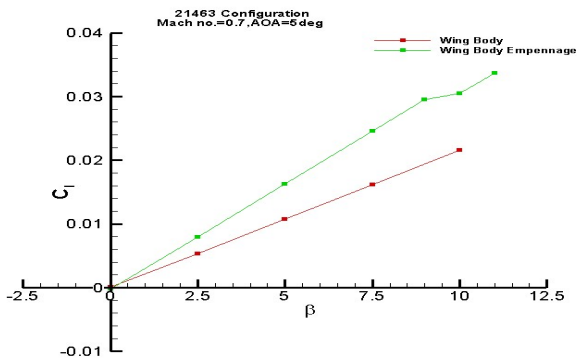


FIGURE: 6.2.2.

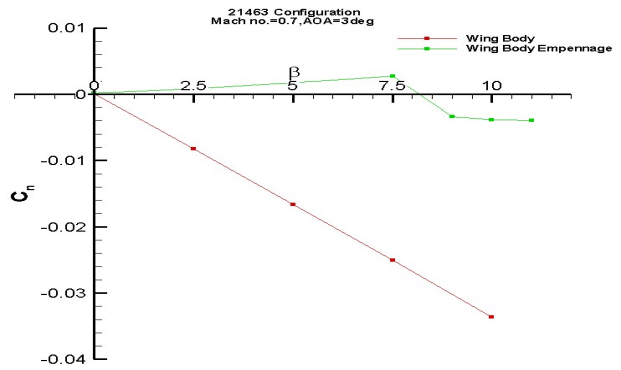


FIGURE: 6.2.3.

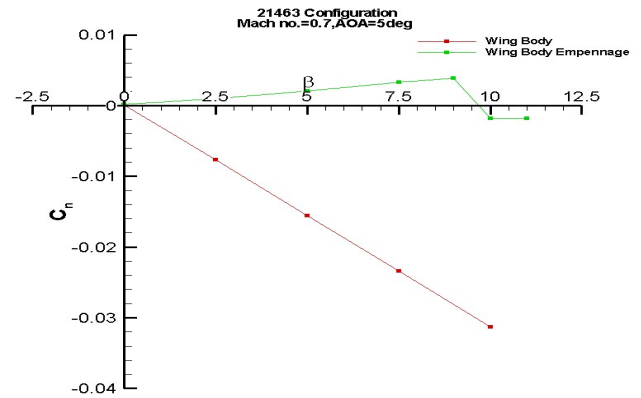


FIGURE: 6.2.4.

The Fig. 6.2.3 and Fig. 6.2.4 explains the C_n - β curve. The fuselage alone usually has destabilising moment which is observed in both curves. The major stability comes from vertical tail as seen from wing-body empennage configuration. The yawing moment increases as the side slip and angle of attack increases till $\beta=7.5^\circ$ and at higher side slip angle, sudden drop in C_n is observed.

The Fig. 6.2.5 and Fig. 6.2.6 shows the Side force (C_y) - β plot. The side force is directly proportional to β as depicted from these curves.

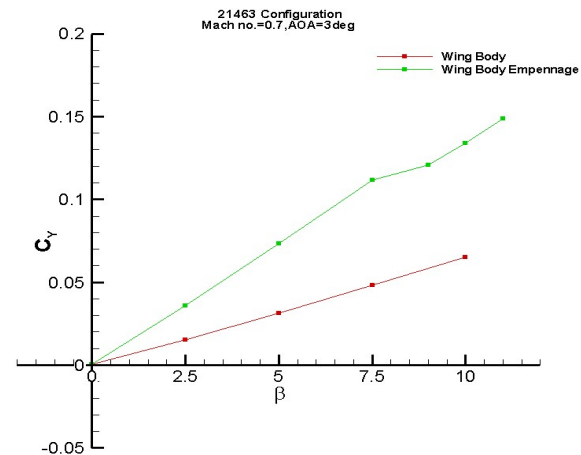


FIGURE: 6.2.5.

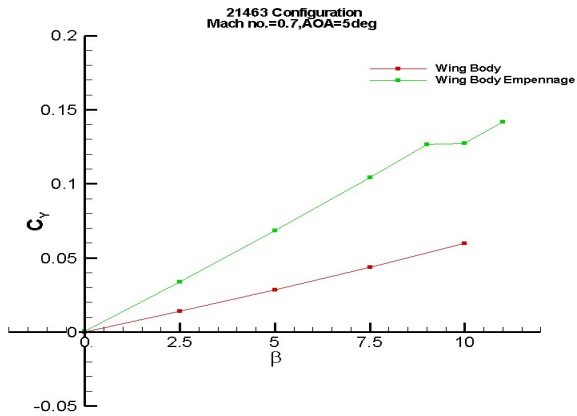


FIGURE: 6.2.6.

CONCLUSIONS

The in-house inviscid Euler code has been widely used for different configuration of RTA-70 aircraft. The asymmetric cases have also produced good results.

The computations have shown the 15.2% improvement in C_L in winglet case over the wing-alone configuration.

It has been found out that the C_{L_0} with respect to C_m increases with Mach Number for wing body and wing body empennage configuration.

The yawing moment increases with the increase in side slip angle till $\beta=7.5^\circ$ beyond which a sharp drop in C_n is observed.

ACKNOWLEDGEMENTS

The author wish to thank Mr. Dilipkumar Ravabawale, Project Engineer for his contributions in pre and post-processing. The authors would like to thank Mr. V.K. Suman, CTFD for carrying out parallelization of Euler code Hyena. The author also wishes to thank Dr. V. Ramesh, Jt. Head, CTFD for technically assessing the CFD work.